Int. J. Heat Mass Transfer. Vol. 21, pp. 137–144. Pergamon Press 1978. Printed in Great Britain

NUCLEATE BOILING HEAT TRANSFER OF LIQUID NITROGEN FROM PLASMA DEPOSITED POLYMER COATED SURFACES

D. F. WARNER,* E. L. PARK, JR and K. G. MAYHAN
University of Missouri—Rolla, Rolla, Missouri, U.S.A.

(*Received* 24 *September* 1976 *and in revised form* 27 *May* 1977)

Abstract—In certain cases, nucleate boiling heat transfer from polymerized tetrafluoroethylene coated surfaces was more than five times the rate of heat transfer found for uncoated surfaces at a given temperature difference. It was also found that for the polymer coated surfaces the transition from nucleate to film boiling was much slower than for uncoated surfaces.

INTRODUCTION

THIS investigation was initiated to determine how an ultrathin coating of plasma deposited tetrafluoroethylene applied to a heat transfer surface affects the nucleate boiling behaviour of liquid nitrogen boiling from the surface.

To the authors knowledge, previous work in this laboratory [1] with plasma deposited polystyrene coated surfaces is the only work concerning plasma deposited polymers as heat-transfer surfaces which has been reported in the literature. Several authors [2–7] have reported data for nitrogen, argon and water boiling from conventional Teflon coated surfaces. It should be pointed out that plasma deposited tetrafluoroethylene polymers are not conventional Teflon. The surface energy of the plasma deposited polymer is much less than conventional Teflon and the polymer is postulated to be extensively crosslinked [8].

* Dr. Warner is now with Union Carbide Co., Charleston, West Virginia, U.S.A.

EQUIPMENT AND EXPERIMENTAL PROCEDURES

The heat-transfer experimental equipment used in this investigation can be catergorized into five separate systems. They are, in order of discussion: pressure control system, electrical system, temperature measuring system, flat plate heater, and heat-transfer surface elements. A schematic diagram is shown in Fig. 1.

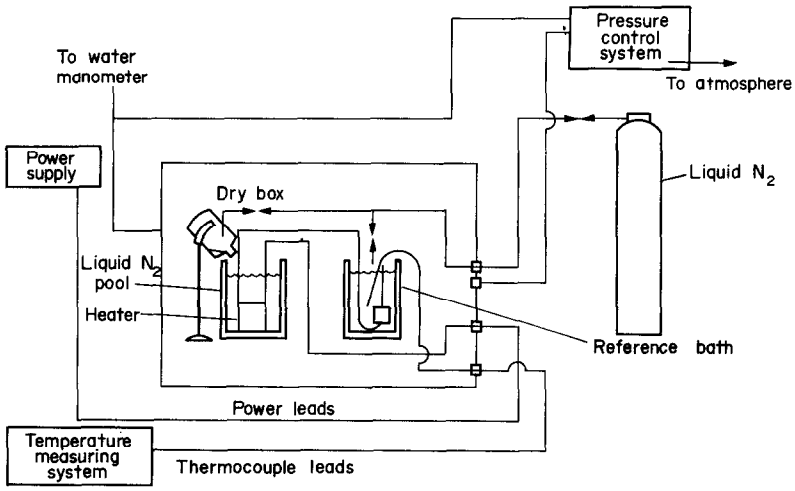

FIG. 1. Schematic diagram of experimental equipment.

The pressure control apparatus consisted of an airtight drybox, a pressure controller-recorder, a pneumatic control valve, a pneumatic differential pressure cell, and a well manometer.

Liquid nitrogen was fed to the drybox from a 110 l Dewar into a 2 l Dewar placed in the drybox. The vaporization of nitrogen in the 2 l Dewar insured a positive pressure inside the drybox at all times. The pressure of the drybox was controlled by bleeding off the nitrogen gas in the drybox through the control valve. The control valve was regulated using a controller and a differential pressure cell. The well manometer was used to determine an accurate pressure in the drybox at all times. The pressure control system

controlled the pressure to within $\pm 249\ N/m^2$ (± 0.1 in of water).

Electrical power was supplied to the heater by two DC power supplies connected in series. The capability of the two supplies with series connection was 0–120 V and 0–40 A. The voltage to the heater was measured with a DC voltmeter to an accuracy of ± 0.1 V. The amperage was measured to an accuracy of 0.025 A with a multi-range ammeter.

and heat flux to be calculated from the thermocouple readings. Two thermocouples were embedded in the center of the disc 0.009 m (0.35 in) apart. The three thermocouples used for temperature distribution calculations were embedded in a triangular shape 0.0254 m (1.0 in) from the center of the disc.

The Teflon insulating shell was machined so that the heater core would slide snugly into it. All thermocouple wires and power leads were run through the

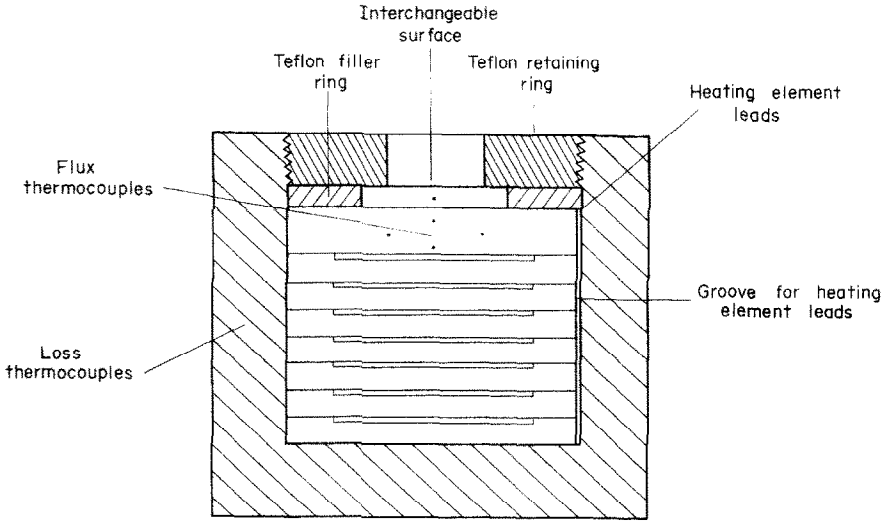

FIG. 2. Flat plate heating device.

The temperature readings were obtained from nine copper–constantan thermocouples leading from the liquid pool and heating device. The thermocouples were distributed as follows: two were used to determine heat losses through the Teflon case from the heating device; five were used to check the heating device thermal flux and radial temperature distribution; one was used to obtain the pool temperature; and one was used to obtain the surface temperature. The thermocouple reference junction was a cold junction compensator. The output from the thermocouples were read with a digital millivoltmeter which was accurate to ± 0.02 mV.

The heating device (Fig. 2), was designed and constructed to accommodate a removable flat plate heating surface with a minimum of heat losses. The heat sources were seven spot heaters 0.0508 m (2 in) in diameter.

The heater core was made of the spot heaters sandwiched alternatively between 0.0762 m (3 in) diameter copper discs approximately 0.0095 m (3/8 in) thick. Each copper disc had a beveled circle in it and a beveled slot for power leads to enable adjacent copper discs to fit flush with each other. High thermal conductivity Insulgrease was used between the copper discs and between the spot heaters and the copper discs to facilitate heat transfer.

The top copper disc was 0.014 m (0.55 in) thick and 0.0762 m (3 in) in diameter. This disc was equipped with five thermocouples to enable heat distribution

top corner of the Teflon. All wires running through the Teflon shell were coated and packed with low thermal conductivity Insulgrease so there would be no liquid leakage around the wires. Two thermocouples were embedded in the Teflon shell to obtain heat flux through the shell. The Teflon was 0.114 m (4.5 in) in diameter and the hole for the heater core was machined so that the bottom of the Teflon shell was 0.019 m (0.75 in) thick. A gold plated heat-transfer element 0.038 m (1.5 in) in diameter and 0.0038 m (0.15 in) thick with an embedded thermocouple was placed on the heating element. High thermal conductivity Insulgrease was placed between the heating element and the heat-transfer element to reduce contact resistance. A 0.019 m (0.75 in) thick Teflon threaded ring with a 0.0254 m (1 in) diameter hole drilled in the center was then screwed into the top of the Teflon shell. The Teflon shell and ring formed an insulation around the entire heating element 0.019 m (0.75 in) thick, the only area free of insulation being an area of 0.0254 m (1 in) in diameter which acted as the heat-transfer surface.

Each heat-transfer surface was made of 0.038 m (1.5 in) in diameter by 0.0038 m (0.15 in) thick electrolytic tough pitch copper. One thermocouple was embedded in each surface in a 0.0014 m (0.056 in) diameter hole drilled from the edge to the center of the surface. The thermocouples were made of 30 gauge thermocouple wire. Each thermocouple was silver soldered together and then soldered into place in the

heat-transfer surface using 60% tin soft solder. The heat-transfer surfaces were then commercially gold plated. The copper surface preparation was done in the same manner for each surface in order to obtain similar surface topography. However, when the surfaces were gold plated, the surface topography was seen to change. Scanning electron micrographs of previous substrates studied in these laboratories [9, 10] have illustrated the differences in surface roughnesses due to changes in current density (position), time, and electroplating bath composition. In this study seven different copper surfaces were electroplated with gold. The thickness of the coating varied from 0.5 to 1.25 μm. The *Rf* plasma reactor used to coat the heat-transfer surfaces with polymer has been described in detail [11, 12]. Therefore this description won't be repeated here.

In these studies each surface was scrubbed with residue free methanol before it was placed in the reactor. The surfaces were then subjected to an argon plasma for 1 h in order to clean submicroscopic particles from the surface. The operating conditions of the plasma generator were then set and the deposition was started.

The controlling variables for the plasma reactor were: power to the *Rf* field, monomer flow rate, position of sample in the reactor, and length of time for deposition. Table 1 shows the operating conditions utilized to prepare each surface coating. All deposition was done at 5 W power to the *Rf* field. The relationship between length of time for deposition and mass of polymer deposited has been shown to be linear [11, 12].

Table 1. Plasma generator operating conditions

Surface	Gold plating thickness (μm)	Polymer thickness (μm)	Reactor position	Power (W)	Deposition rate
1	0.5	2	11 & 12	5	0.08 μg/h
3	0.5	2	13 & 14	5	0.08 μg/h
4	0.5	4	7 & 8	5	0.08 μg/h
5	0.5	8	11 & 12	5	0.08 μg/h
8	0.5	6	11 & 12	5	0.08 μg/h
11	0.75	4	11 & 12	5	0.08 μg/h
12	1.25	6	11 & 12	5	0.08 μg/h

It should be emphasized that tetrafluoroethylene deposited in an *Rf* plasma yields a surface which has a lower surface free energy than conventional Teflon.

RESULTS AND DISCUSSION

All surfaces were examined with a scanning electron microscope (micrographs were taken at 200× and 2000×) before the coating was applied, after the coating was applied, and after boiling had occurred from the surface. The portion of the surface which was insulated by the Teflon retaining ring and that portion which contacted the liquid nitrogen during boiling were both examined after boiling had occurred. The two portions of the heat-transfer surface underwent the same temperature extremes and environmental changes with the exception of the boiling of liquid nitrogen which did not occur on the surface protected by the Teflon ring. It is, therefore, felt that any difference between the two sections of the surface is due to the boiling action of the liquid nitrogen. For an analysis and detailed discussion of the micrographs the reader is referred to [13].

It is recognized that each of the heat-transfer surfaces will give a slightly different boiling curve, therefore, a series of curves were obtained based on data from three uncoated heat-transfer surfaces (see Fig. 3) and reference curves were derived from these data. Data for surface 7 fell between the data for surface 2 and surface 4 with approximately 15% relative deviation. Data for any particular surface will yield a different curve. However, the data at lower fluxes is nearly the same for all gold plated surfaces. Therefore, two lines have been drawn which bracket the data. The area between these two lines is considered as representative of nitrogen boiling from flat plate heat-transfer surfaces which are made of copper plated with gold.

Surfaces 1, 3, 4, 5, 8, 11, and 12 were coated with varying thicknesses of TFE plasma deposited polymer as shown in Table 1. Data were then obtained which determined the respective nucleate boiling curve for each of the surfaces.

Surface 1 was coated with TFE approximately two microns thick. Its boiling curve (Fig. 4) shows no deviation from the reference boiling curve although larger ΔT's were obtained with this surface before burnout occurred. When the micrographs of surface 1 were examined, it was seen that the polymer surface had failed. This failure could have occurred during the aging process before any nucleate boiling data was taken or it could have resulted from the initial boiling run. As a result of the aging procedure, the exposed surfaces were subjected to boiling during cooldown. There was no noticeable shift in the data of succeeding runs on this surface indicating that after the initial failure the surface was stable during succeeding boiling runs.

Surface 3 was coated with TFE approximately two microns thick but under slightly different polymerization conditions than were used for surface 1. Its boiling curve (Fig. 4) is shifted upward from that of

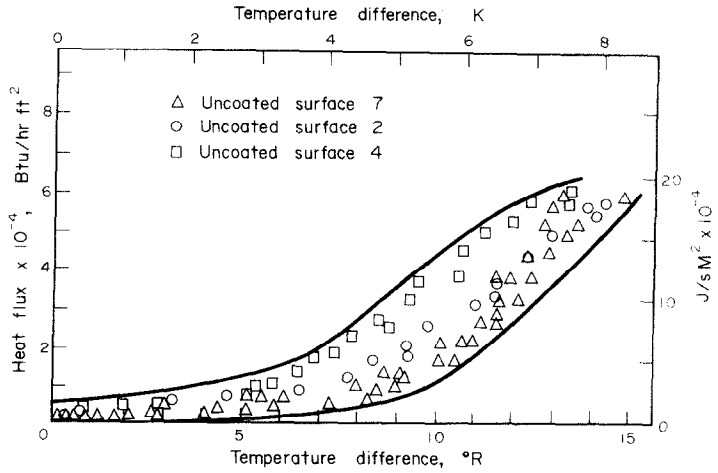

FIG. 3. Nucleate boiling of gold plated copper surfaces.

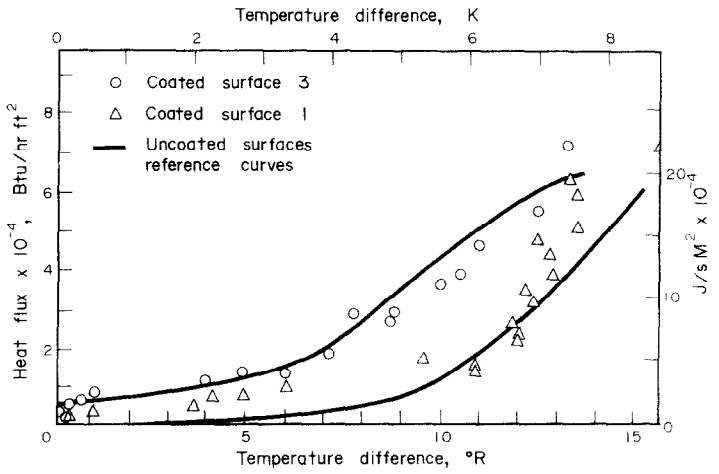

FIG. 4. Comparison of the nucleate boiling behaviour of 2 μm coated surfaces and uncoated surfaces.

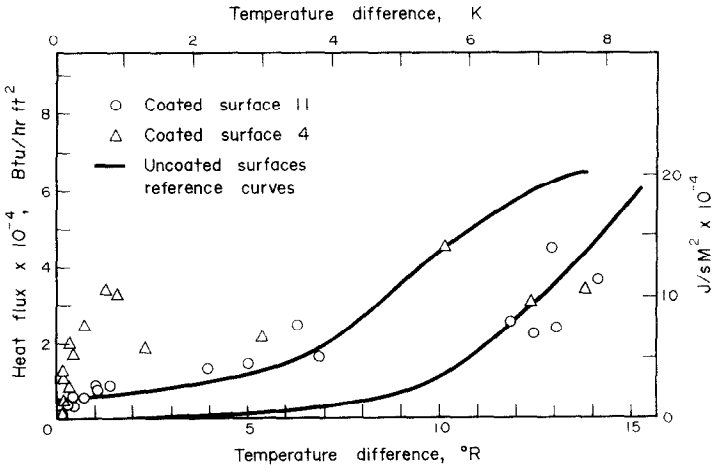

FIG. 5. Comparison of the nucleate boiling behaviour of 4 μm coated surfaces and uncoated surfaces.

surface 1 and falls at the upper limit of the area which brackets the boiling range for gold plated heat-transfer surfaces. The micrographs of surface 3 show that the surface did not fail as did surface 1, which may account for the shift upward in the boiling curve. Micrographs of this surface show little if any change in the surface due to boiling. It can also be seen from the micrographs of the surface before and after the polymer coating was applied, that the surface was smoothed considerably, due to the coating. The initial gold plated surface was, however, smoother than surface 1.

Surface 11 was coated with TFE approximately 4 μm thick. The boiling curve (Fig. 5) for this surface shows a shift upward from the reference curve at low fluxes but the curve flattens out at higher fluxes to yield results similar to those obtained with an uncoated surface.

Surface 4 was used to obtain data for the reference curve for uncoated surfaces. It was then coated with TFE approximately 4 μm thick. The boiling curve (Fig. 5) drawn from data taken after the polymer coating was applied indicates a shift in the curve somewhat similar to surface 11. However, the initial shift of the boiling curve upward is much more pronounced than it was with surface 11. The micrographs of surface 4 indicate that the surface had failed in a manner similar to surface 1. Non-dispersive X-ray patterns of surface 4 indicated that there was still polymer covering the entire surface and the surface was still much smoother than a reference surface even after failure.

It should be noted that coating in position 7 and 8 in the reactor will tend to give a slightly thicker coating than coating in position 11 and 12. The fact that surface 11 was coated in position 11 and 12 while surface 4 was coated in position 7–8 may partially explain the difference in their boiling curves (see Table 1).

Surface 8 was coated with TFE approximately 6 μm thick. The nucleate boiling curve (Fig. 6) is shifted upward considerably from the curves that would be expected for an uncoated surface.

Surface 12 was coated with TFE approximately 6 μm thick. The boiling curve for surface 12 (Fig. 6) is shifted upward similar to the curve for surface 8 at low fluxes, however as the flux increases the curve flattens out at high fluxes and behaves as an uncoated surface would. Examination of the micrographs for surface 12 showed that the surface had failed in a manner similar to surface 1 and 4. However, an examination of the surface by non-dispersive X-ray techniques reveals that there was still polymer covering all parts of the surface including the spots where the coating failed. This failure may account for the different behaviour between surfaces 8 and 12. It is interesting to note that surfaces 1, 4, and 12 which failed show similar results at high temperature differences.

Surface 5 was coated with TFE approximately eight microns thick. This surface yielded the most reproducible boiling data of any of the TFE coated surfaces studied (Fig. 7). Again, all changes in the boiling surface appeared to occur prior to or during the aging process. The less than 2% scatter in most of the data was probably due to the preponderance of good nucleation sites which can be seen in the micrographs of this surface. The curve has been greatly shifted from the reference curve. The boiling curve indicates that at moderate heat fluxes, more than five times as much heat was transferred through surface 5 as through the reference surfaces at the same ΔT. A similar phenomena was also observed by Young and Hummel [4–6], who boiled water from linear Teflon.

It should be noted that the polymer coating on surface 5 was deposited over a period of 96 h. The micrographs of the surface after boiling show that the surface was eroded in an irregular furrowed pattern. There were no obvious failures in the coating of the type discussed with respect to surface 1, 4, and 12. Adhesion to the substrate appeared to be unaffected by the boiling process.

A comparison of the effect of polymer film thickness on the boiling curve indicated that as the polymer coating was made thicker, the initial portion of the curve was shifted further away from the reference curve. It should be noted that the polymer coated surfaces yield a lower temperature difference for a given heat flux; therefore, the heat transfer is more efficient. If thicker polymer films possessing the characteristics found in surface 5 can be reproduced, improved nucleate boiling surfaces can be produced.

While taking data using polymer coated surfaces it was noticed that the time it took a coated surface to go through the critical flux and enter film boiling was much greater than for an uncoated surface. The surface temperature was recorded at one minute intervals for both a polymer coated surface an an uncoated surface and the results are shown in Fig. 8.

The results of the above tests indicate that the high temperature differences between the heat-transfer surface and the liquid pool which occur in film boiling can be avoided with a polymer surface because there is time to reduce the power input to the heater before destructively high temperatures are reached on the surface.

Clark, Strenge and Westwater [14] and Preckshot and Denny [15, 16] found that active cavity site dimensions varied from 25 μm (0.001 in) to 5 μm (0.0002 in) in diameter. Electron micrographs of surfaces 3, 8 and 11 indicate the largest cavities present on these surfaces are at least a factor of one hundred smaller than those previously described, yet nucleation readily occurred on these surfaces. The possible explanation for the large active cavity sizes postulated in the papers cited above is that the bubbles form inside the larger nucleation sites rather than at the mouth of the cavity. The above investigators did not have access to an electron microscope, and it was, therefore, impossible for them to determine whether they had smaller nucleation sites within their larger nucleation sites. If inception of boiling occurred at smaller sites within the larger sites, the bubble would migrate upward as it grew and fill the larger site, giving the

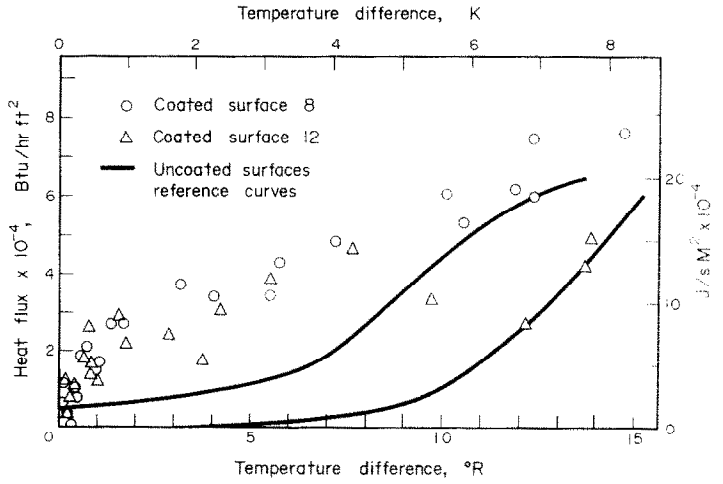

FIG. 6. Comparison of the nucleate boiling behaviour of 6 μm coated surfaces and uncoated surfaces.

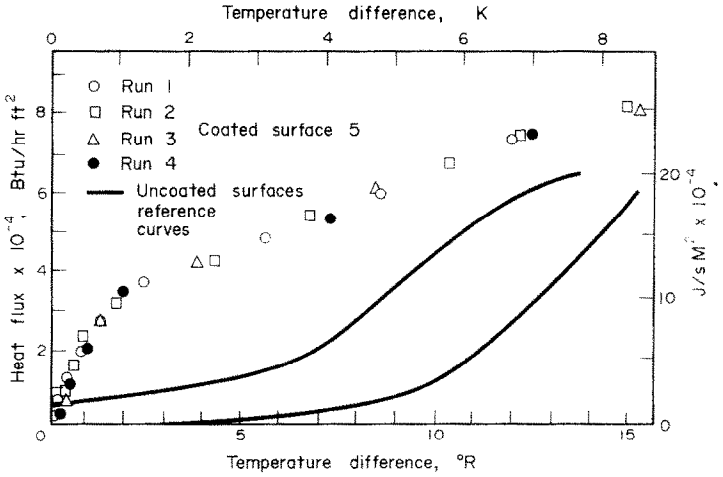

FIG. 7. Comparison of the nucleate boiling behaviour of 8 μm coated surfaces and uncoated surfaces.

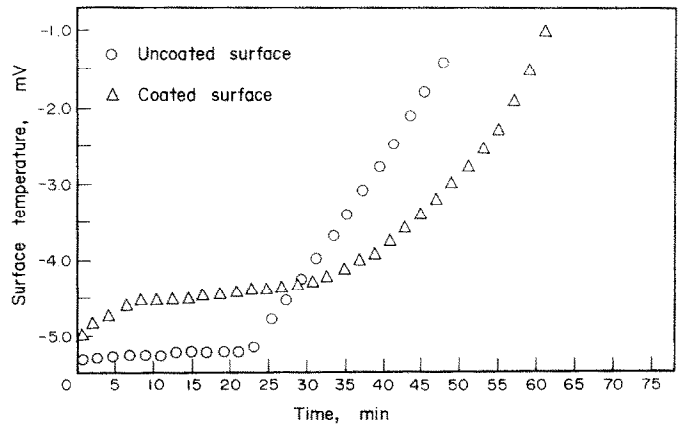

FIG. 8. Comparison of the rate of burnout for a polymer coated and uncoated surface.

visual impression that the bubble had initiated at the mouth of the larger site.

In order to consider, in depth, the boiling phenomenon from very small nucleation sites it is first necessary to study the forces acting on a bubble as it forms. When a bubble first forms, it is held to the surface of the heater by the interaction between the bubble wall and the heater surface. As the bubble grows, the buoyancy of the bubble becomes greater until the bubble wall–surface interactions are overcome, at which time the bubble breaks loose from the surface and rises to the surface of the liquid. The interaction of the bubble wall and the boiling surface is partially controlled by the perimeter of the cavity in which the bubble forms. It then follows that a large cavity would produce a large bubble since a large amount of buoyancy is required to overcome the bubble wall–surface interaction and likewise a small cavity would foster a smaller bubble.

Carr [17], using knurled surfaces observed that at low fluxes bubbles formed on or close to the points of the knurled surface and then migrated to the bottom of the knurl where the bubble wall–surface contact was greatest. This bubble migration effect could also explain how a bubble can form at a minute spot on the side of a large cavity and then migrate to the bottom of the cavity as it grows where the bubble wall–surface contact is greatest. As pointed out by Carr, the bubble would move to the position that offers a maximum microlayer area/bubble volume ratio.

The micrographs taken of the boiling surfaces 3, 8, and 11 indicate that all nucleation sites are on the order of 1 μm (4×10^{-5} in) or less. Cavities of these small dimensions should yield very small bubbles which in fact was the case. Also surfaces which have no large cavities will have more nucleation sites which are actively producing bubbles since a large cavity could contain several small cavities but produce only one bubble at a time.

The theory of much smaller cavities acting as nucleation sites is further substantiated by examining the boiling data from the TFE coated surfaces. It can be seen from the data that, as the polymer coating becomes thicker, the boiling curve shifts further away from the reference curve showing that more heat is transferred at lower temperature differences. This phenomena is understandable if one considers what happens to the topography of the surface as the coatings become thicker. It was shown from the scanning electron microscope study of the surfaces that as the polymer coating became thicker, the surfaces became smoother. As the surfaces become smoother, the possibility of one nucleation site shadowing another decreases since the nucleation sites approach the same relative size. This lack of shadowing of nucleation sites allows more nucleation sites to be independently active and thus more bubbles form. With this greater preponderance of bubbles forming, more heat can be transferred from the surface at a lower temperature difference.

The transient data taken at or above the burnout flux also indicates that the bubbles are forming independently of each other. In order for a vapor film to form over a heat-transfer surface, the surface must be hot enough to immediately vaporize the liquid on the surface, or the bubbles must be forming close enough together or be large enough to interact with each other. Small nucleation sites will support only small bubbles as previously described. Therefore the bubbles are not large enough (if the nucleation sites are far enough apart) to interact with each other and form a film at normal burnout fluxes. This lack of interaction of the bubbles explains the large heat fluxes at low temperature differences observed in this study. It is also felt that the inability of the bubbles to interact with each other and support a vapor film is responsible for the length of time that was observed for the surface to enter film boiling.

CONCLUSIONS

The following conclusions were drawn as the result of this investigation:

1. Active nucleation sites were found to be much smaller than had previously been reported in the literature.
2. Surfaces coated with plasma deposited TFE will transfer heat more efficiently than uncoated surfaces.
3. Surfaces coated with plasma deposited TFE go through the critical heat flux into film boiling at a rate which is much slower than the rate which uncoated surfaces exhibit for this same transition.

Acknowledgements—The authors would like to acknowledge the following organizations for financial assistance during this investigation, Phillips Petroleum Company and Atlantic Richfield Company.

REFERENCES

1. D. F. Warner, E. L. Park and K. G. Mayhan, The effect of nucleate boiling on polystyrene-coated surfaces, *Adv. Cryog. Engng* **17**, 414 (1972).
2. C. B. Cobb, A study of surface and geometric effects on the nucleate boiling of liquid nitrogen and liquid argon from atmospheric to the critical pressure, Ph.D. Thesis, University of Missouri—Rolla (1967).
3. C. B. Cobb and E. L. Park Jr., Nucleate boiling—a maximum heat flux correlation for corresponding states liquids, *in Heat Transfer Chem. Engng Prog., Symp. Ser.* **65**, 188 (1969).
4. R. K. Young and R. L. Hummel, Heat transfer performance of surfaces with artificial nonwetted sites, *Can. J. Chem. Engng* **46**, 299 (1968).
5. R. K. Young and R. L. Hummel, Improved nucleate boiling heat transfer, *Heat Transfer, Chem. Engng Prog., Symp. Ser.* **61**, 46 (1965).
6. R. K. Young and R. L. Hummel, The burnout of surfaces having precise arrays of active sites, Presented at the 10th National A.I.Ch.E.—A.S.M.E. Heat Transfer Conference, Philadelphia (August 1968).
7. P. J. Marto, J. A. Moulson and M. D. Maynard, Nucleate pool boiling of nitrogen with different surface conditions, *J. Heat Transfer* **90**, 437 (1968).
8. L. F. Thompson and K. G. Mayhan, The design, construction, and operation of an inductively coupled

plasma generator and preliminary studies with nine monomers, *J. Appl. Polym. Sci.* **16** (9), 2291–2315 (1972).
9. D. V. Porchey, E. L. Park and K. G. Mayhan, A scanning electron microscope surface study of nucleate pool boiling heat transfer to saturated liquid nitrogen, *A.I.Ch.E. Symposium Series* **68**, 162–171 (1972).
10. D. V. Porchey, An SEM, surface study of nucleate pool boiling heat transfer to saturated liquid nitrogen at reduced pressures from 0.1 to 0.9, Ph.D. Thesis, University of Missouri–Rolla, Rolla, Missouri (1970).
11. L. F. Thompson and K. G. Mayhan, The design, construction, and operation of an inductively coupled plasma generator and preliminary studies with nine monomers, *J. Appl. Polym. Sci.* **16** (9), 2291–2315 (1972).
12. L. F. Thompson, Ph.D. Thesis, University of Missouri–Rolla, Rolla, Missouri (1970).
13. D. F. Warner, Nucleate boiling from polymer coated surfaces, Ph.D. Thesis, University of Missouri–Rolla, Rolla, Missouri (1973).
14. H. B. Clark, P. S. Strenge and J. W. Westwater, Active sites for nucleate boiling, *Heat Transfer, Chem. Engng Prog., Symp. Ser.* **55**, 103 (1959).
15. V. E. Denny and G. W. Preckshot, Explorations of surface and cavity properties on the nucleate boiling of carbon tetrachloride, *Can. J. Chem. Engng* **45**, 241–246 (1967).
16. V. E. Denny, Some effects of surface micro-geometry on natural convection and pool boiling heat transfer to saturated carbon tetrachloride, Ph.D. Thesis, University of Minnesota (1961).
17. J. J. Carr, The effect of a knurled heat transfer surface upon pool nucleate boiling of normal pentane, Ph.D. Thesis, University of Missouri–Rolla, Rolla, Missouri (1971).

TRANSFERT THERMIQUE PAR EBULLITION NUCLEEE D'AZOTE LIQUIDE CONTRE UNE SURFACE RECOUVERTE D'UN POLYMERE DEPOSE PAR PLASMA

Résumé—Dans certains cas, le transfert thermique par ébullition nucléée à des surfaces recouvertes de tétrafluoroéthylène polymérisé est cinq fois plus grand que pour des surfaces nues avec la même différence de température. On trouve aussi que pour les surfaces couvertes de polymère, la transition entre ébullition nucléée et ébullition en film est plus lente que pour les surfaces nues.

WÄRMEÜBERGANG BEIM BLASENSIEDEN VON FLÜSSIGEM STICKSTOFF AN PLASMAGESPRITZTEN, POLYMERBESCHICHTETEN OBERFLÄCHEN

Zusammenfassung—In gewissen Fällen ergab der Wärmeübergang beim Blasensieden an mit Tetrafluoräthylen beschichteten Oberflächen 5 mal so hohe Werte wie der an unbeschichteten Oberflächen bei gleicher Temperaturdifferenz ermittelte. Außerdem wurde gefunden, daß bei polymerbeschichteten Oberflächen der Übergang vom Blasen- zum Filmsieden viel langsamer als bei unbeschichteten Oberflächen vonstatten ging.

ПЕРЕНОС ТЕПЛА С ПОЛИМЕРИЗОВАННЫХ ПОВЕРХНОСТЕЙ ПРИ ПУЗЫРЬКОВОМ КИПЕНИЙ ЖИДКОГО АЗОТА

Аннотация — В некоторых случаях при пузырьковом кипении скорость переноса тепла от покрытых четырехфтористым этиленом поверхностей в 5 раз превышала скорость теплопереноса по сравнению с неполимеризованными поверхностями при данной температурной разности. Найдено также, что для полимеризованных поверхностей переход от пузырькового кипения к пленочному происходит гораздо медленнее, чем в случае неполимеризованных поверхностей.